Effect of shell thickness on the deformation mode of TPMS lattices in quasi-static compression

WCMNM 2021

Jin Fu[a], Lei Zhang[b], Xu Song[c,*], Mingwang Fu[a,*]

a Department of Mechanical Engineering, The Hong Kong Polytechnic University, Hung Hom, Kowloon, Hong Kong

b Department of Mechanical and Aerospace Engineering, Hong Kong University of Science and Technology, Clear Water Bay, Kowloon, Hong Kong

c Department of Mechanical and Automation Engineering, Chinese University of Hong Kong, Shatin, Hong Kong

∗ Contact authors: xsong@cuhk.edu.hk (Xu Song); mmmwfu@polyu.edu.hk (M.W. Fu)

Abstract

Triply periodic minimal surface (TPMS) shell-like structures are gaining increasing attention due to their light-weighting potential as well as the energy absorption capability. Decreasing shell thicknesses of TPMS is necessary for further lightweighting, where micro additive manufacturing (AM) can well satisfy the increasing fabrication precision. However, the deformation mode of TPMS structures could be different due to the reduction of shell thicknesses. Finite element (FE) modelling was conducted in this work to study the deformation mode and mechanical properties of TPMS structures considering the effect of multi-scale shell thicknesses. Three typical TPMS structures, i.e. Primitive (P), Diamond (D) and Gyroid (G) surfaces, were designed and their compression behaviours were simulated. It is found that smaller shell thickness results in obvious stress fluctuation during plateau region, while higher thickness leads to continuous hardening effect. With shell thickness increases, the compressive deformation mode transforms from localized collapse of TPMS layers to homogenously bulk deformation. TPMS structures with higher shell thickness correspond to higher stiffness, strength and energy absorption ability. Among the three TPMS geometries, D-type structure shows greater potential for energy absorption application. Overall, this numerical study provides an understanding of the deformation mechanism of TPMS structures with multiscale shell thicknesses. Besides, it may offer a guideline for practical TPMS design and manufacturing, as well as tuning of their mechanical properties.

Keywords: TPMS, micro additive manufacturing, finite element modelling, deformation mode, shell thickness

1. Introduction

Triply periodic minimal surface (TPMS) shell-like structures are showing great attraction in many applications, such as light-weighting design, heat exchanger, tissue engineering and energy absorption [1]. They exhibit zero mean curvature and continuous surface. In terms of mechanical property, it is reported that TPMS structures demonstrate reduced stress concentration, higher strength and better energy absorption capability over strut-based lattice structures [2, 3]. Therefore, TPMS structures are promising for light-weighting mechanical applications.

Thanks to additive manufacturing (AM), such as selective laser melting (SLM), TPMS structures with such complicated geometry can be easily fabricated, which is almost impossible using conventional fabrication technologies. SLM has been successfully used to fabricate TPMS structures from various metallic powders [3-5]. In order to achieve further lightweighting, shell thickness of TPMS must be further reduced to lower the structure relative density. Besides, micro SLM system has been developed to satisfy the higher fabrication precision [6].

Due to possible effect of shell thickness, the TPMS structures with micro-scale shell thickness may demonstrate different mechanical behaviour. In the current scope, it is well-known that the relative density affects the mechanical performance, such as stiffness, strength and energy absorption. However, the effect of shell thickness on the deformation mode of TPMS structures has been rarely studied to the authors' knowledge.

Before time-consuming and expensive experimental study, finite element (FE) analysis is conducted firstly in this work. Typical TPMS structures with various thicknesses are designed, and the compressive behaviour as well as the mechanical properties are simulated and analysed. Experimental study will be conducted to validate the FE models as future work.

2. Modelling procedures

2.1. Design of TPMS

TPMS model can be described using implicit nodal approximation. In this work, Primitive (P), Diamond (D) and Gyroid (G) surfaces are selected, which can be generated using the following implicit functions [7]:

$$\emptyset_P = cos(wx)+cos(wy)+cos(wz) = c$$
$$\emptyset_G = cos(wx)sin(wy)+cos(wy)sin(wz)+ cos(wz)sin(wx) = c$$
$$\emptyset_D = sin(wx)sin(wy)sin(wz)+sin(wx)cos(wy)cos(wz)+ cos(wx)sin(wy)cos(wz)+cos(wx)cos(wy)sin(wz) = c$$

where *x, y, z* are spatial coordinates, $w=2\pi/L$ and *L* is the unit cell size. The level c controls the shape of the unit cell, as well as the surface area of the TPMS.

The G-, D-, P-type TPMS models are created by extracting surfaces using the above equations with c defined as zero. Matlab script is used to generate the 3D stereo-lithography (STL) models of TPMS structures. It should be noted that the surface mesh of the TPMS generated by Matlab code is of poor quality. Hypermesh software is used to remesh the TPMS for subsequent FE analysis. The extracted G-, D-, P-type models comprising of 4×4×4 unit cells are shown in Fig. 1. The unit cell length is defined as 4 mm, thus, the size of each structure is 16×16×16 mm.

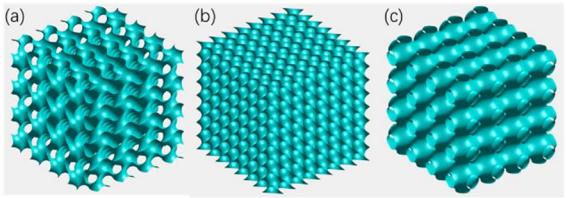

Fig. 1 3D models of TPMS structures: (a) G, (b) D and (c) P

2.2 Finite element modelling

The compressive responses of the G-, D-, P-type TPMS are analysed using FE package Abaqus/Explicit 2017. The material property of 316L stainless steel produced by SLM is used for FE modelling with isotropic hardening. The true stress-plastic strain curve of the base material is shown in Fig. 2. The Young's modulus and Poisson's ratio are 190GPa and 0.3, respectively. No failure model is used since the sheet failure is proved not evident after the onset of densification [3].

The TPMS is modelled using triangular shell elements of type S3 with an average element size of 0.2mm. According to our previous mesh sensitivity study, compared with 0.1 mm, the element size 0.2 mm can not only have similar FE results but also save computation expense. Two rigid plates are modelled and placed on the top and bottom of the TPMS structure. All degrees-of-freedom of the bottom plate are fixed, and the top plate is moved down with a strain rate of $0.001s^{-1}$. General hard contact is assigned for the assembly. Mass scaling was applied to ensure a minimal stable time of 5×10^{-4} s for each increment.

Since varying shell thickness leads to different relative density (ρ_r) of the TPMS, four levels of ρ_r are selected, i.e. 5%, 10%, 20%, 40%. The shell thickness can be calculated by $t = V_{cube} * \rho_r / S_{TPMS}$. V_{cube} is the volume of the cube. S_{TPMS} is the surface area and can be measured from the 3D STL model. The thicknesses of the TPMS structures are illustrated in Table 1.

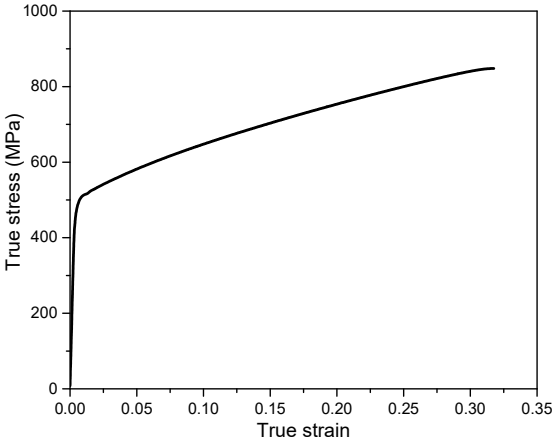

Fig. 2 The true stress-plastic strain curve of 316L stainless steel produced by SLM

Table 1 Shell thickness of the TPMS structures

Type \ ρ_r	5%	10%	20%	40%
G	0.065	0.129	0.258	0.516
D	0.052	0.104	0.207	0.414
P	0.085	0.170	0.339	0.678

3. Results and discussion

3.1 Stress-strain curves

Fig. 3 shows the numerical stress-strain curves of all TPMS structures. In general, the predicted stress-strain responses can correctly capture the three typical deformation stages of TPMS structures, i.e. linear elastic deformation region, and stress plateau region followed by densification region. In the plateau region, the unit cell collapses by yielding, and the stress keeps almost constant during a wide strain region. Noted that the energy absorbed during the plateau region is an important indicator for energy absorption application. In the third stage, the structure deforms like a solid material after all layers collapse and fully contact with each other, accompanied with evident strain hardening effect.

For larger shell thickness, the TPMS structures show higher strength and continuing stress hardening effect, which are caused by more rapid contact and densifying of the collapse of the TPMS layers. The D-type TPMS with 40% density shows the most significant hardening effect during compression.

For smaller shell thickness, i.e. lower relative density (below 20%), the strength of the structure decreases upon structure yielding after linear elastic region. The softening effect may be attributed to the abrupt shear band failure [4]. Subsequently, the stress-strain curves exhibit fluctuations for a wide strain range until the densification of the structure, which is caused by localized buckling of curved walls.

Among the three types of TPMS, G-type structure shows the least stress fluctuations and relatively stable stress-strain behavior. P-type shows unstable and intensive stress variation during plateau region. This geometrical dependent difference can be explained by the internal material distribution, which affects the load-bearing capacity of the structure. Since the internal material distribution of P-type structure is relatively heterogeneous, the load-bearing capacity along loading direction is non-uniform, leading to unstable fluctuating region [4]. Interestingly, for the lowest density of D structure, there are several distinct stress peaks and valleys, where each of them may correspond to the collapse of one sub-layer. Besides, the stress peaks of P structure gradually increase during the plateau region. The hardening effect is due to the gradual densification of the collapsed layers [8].

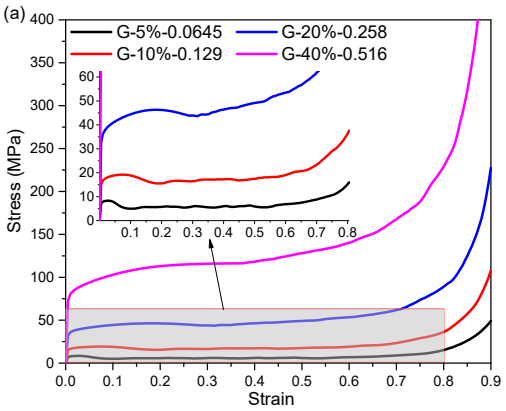

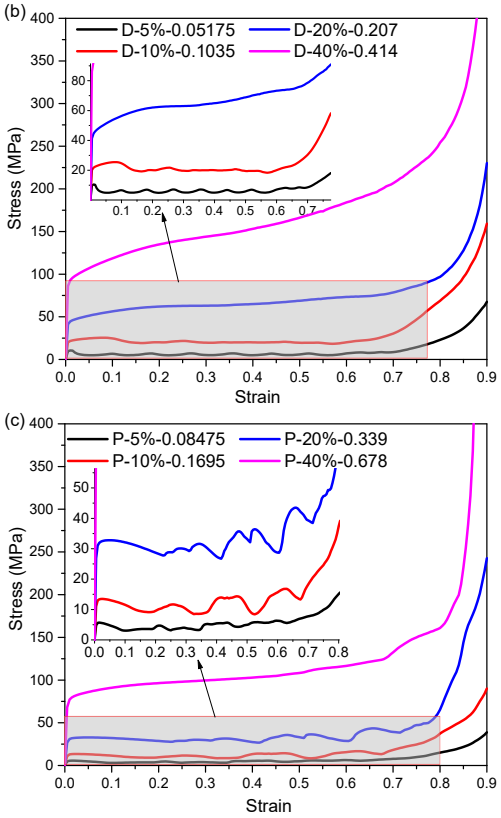

Fig. 3 Numerical stress-strain curves of (a) G-, (b) D-, (c) P-sheet structures with different thicknesses

3.2 Deformation mode analysis

Fig. 4 shows the stress distribution within the structures at different strains. It is found that the deformation characteristics are dependent on the shell thickness, namely the relative density of the structure. In general, for lower shell thickness, the internal stress is non-uniformly distributed within the structure, representing localized deformation and collapse. With shell thickness increasing, the stress distribution becomes more uniform. The deformation mode transforms from localized mode to bulk deformation behavior, which shows continuous hardening effect without significant stress fluctuation. In addition, it is found that the densification strain of the TPMS structures decreases with increasing shell thickness, because of the earlier compact of the crushed layers with larger shell thickness.

For G-type TPMS of lower relative density (5% and 10%), the structure crushing is heterogeneous and concentrated at the central layers before densification. For D-type TPMS, the structure with the smallest thickness shows a distinct layer-by-layer crushing behavior, where each layer collapse corresponds to one stress peak and valley on the stress-strain curve during plateau region. The D-type structure with 20% density also shows a localized deformation behavior. Specifically, P-type structure at lower relatively density deforms and collapses by diagonal shear, demonstrating double shearing bands, as shown in Fig. 4(c). The failure of diagonal layers leads to significant heterogeneous stress distribution during the plateau region. This is because the unique P-type structure has significant non-uniform internal material distribution, leading to heterogenous load-bearing capacity.

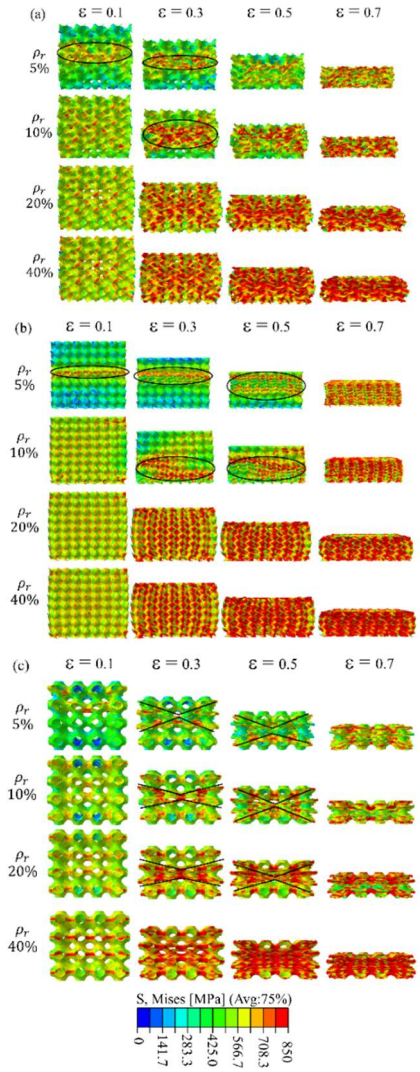

Fig. 4 FE stress plots at given strains of (a) G-, (b) D-, (c) P-sheet structures

3.3 Mechanical property

As the mechanical property of TPMS is orientation dependent, the loading direction parallel to the <100> direction of TPMS is considered in this work. The mechanical properties of these structures are extracted from the numerical stress-strain curves. The Young's modulus *E* is calculated as the slope of the linear stage. The plateau stress σ_{pl} is determined as the mean stress ranging from 0.2 to 0.4 strain [9]. The energy absorbed per unit volume *W* is defined as the area under the stress-strain curve up to 50 % strain [9]. Based on the theoretical work by Gibson and Ashby, normalized *E*, σ_{pl} and *W* are utilized to compare and analyze the mechanical properties of the TPMS structure, which are expressed as:

$$\frac{E}{E_S} = C1 * {\rho_r}^{n1}, \frac{\sigma_{pl}}{\sigma_y} = C2 * {\rho_r}^{n2}, \frac{W}{\sigma_y} = C3 * {\rho_r}^{n3}$$

where E_S and σ_y are Young's modulus and yield strength of the base material. The coefficients C_1, C_2, C_3 and exponents n_1, n_2, n_3 differ for different geometries of TPMS. Fig. 5 shows relationship between the normalized mechanical property and relative density, as well as the fitted equations.

All of the three mechanical property indexes increase with the relative density, following certain positive power relationship. The fitted exponents $n1$

and $n2$ fell within the range of [0.1, 4] and [0.1, 1] for modulus and strength, respectively, which are predicted by analytical modeling of Gibson-Ashby [10]. The D-type TPMS shows the highest compressive modulus than G- and P-type structures. The fitted exponent of modulus for P-type structure is 1.27, which is higher than the other two. This indicates that the stiffness of P-type structure decreases at a higher speed during light-weighting process, showing a disadvantage over the other two structures. The fitting exponents n_2 and $n3$ for strength and energy show similar level among the three types of TPMS. Besides, D-type structure shows the highest plateau stress, as well as the best energy absorption capability. As a result, D-type structure shows greater potential for energy absorption application as compared with G- and P-type structures. The mechanical properties and their scaling behaviors in this simulation work are comparable to those reported in [3].

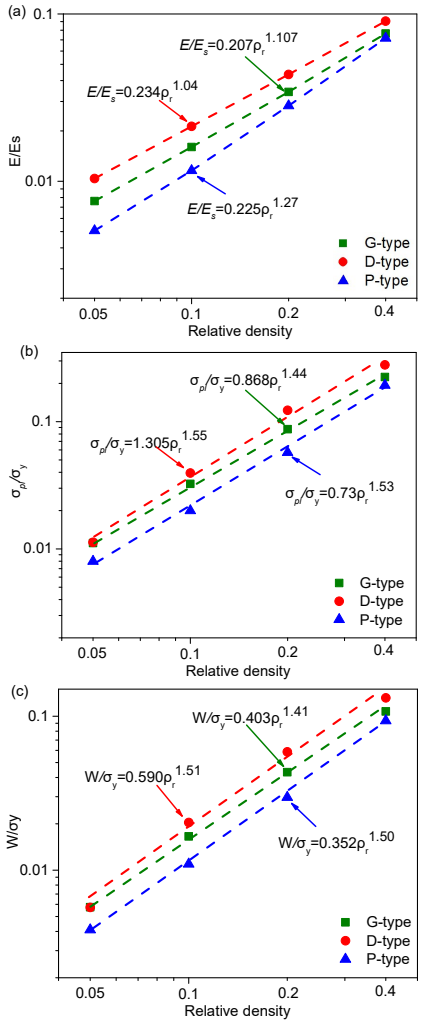

Fig. 5 Normalized mechanical properties with respect to relative density: (a) compressive modulus, (b) plateau stress, (c) energy per unit volume

4. Conclusions

In this work, FE analysis was conducted to study the deformation behaviour of TPMS structure with the effect of shell thickness taken into consideration. The stress-strain response, deformation mode as well as the mechanical properties were analysed. The main findings are as follows:

(1) TPMS structures with small shell thickness (low relative density) show stress fluctuation during plateau region, while higher thickness leads to continuous hardening effect.

(2) With shell thickness increasing, the deformation mode transforms from localized collapse of TPMS layers to bulk deformation of the whole structure before densification.

(3) TPMS structures with higher shell thickness correspond to higher stiffness, strength and energy absorption ability. D-type structure shows greater potential for energy absorption application.

Moreover, the FE models should be validated by comparing with experimental results. A series of TPMS structures will be fabricated, and related compressive tests will be conducted to validate the predicted results in the future work.

Acknowledgements

FU Jin and MW Fu would like to acknowledge the financial support from The Hong Kong Polytechnic University (NO. 1-ZVMR and BBAT).

References

[1] T. Maconachie, M. Leary, B. Lozanovski, X. Zhang, M. Qian, O. Faruque, M. Brandt, SLM lattice structures: Properties, performance, applications and challenges, Mater. Des. (2019) 108137.

[2] I. Maskery, N.T. Aboulkhair, A. Aremu, C. Tuck, I. Ashcroft, Compressive failure modes and energy absorption in additively manufactured double gyroid lattices, Addit. Manuf. 16 (2017) 24-29.

[3] L. Zhang, S. Feih, S. Daynes, S. Chang, M.Y. Wang, J. Wei, W.F. Lu, Energy absorption characteristics of metallic triply periodic minimal surface sheet structures under compressive loading, Addit. Manuf. 23 (2018) 505-515.

[4] M. Zhao, D.Z. Zhang, F. Liu, Z. Li, Z. Ma, Z. Ren, Mechanical and energy absorption characteristics of additively manufactured functionally graded sheet lattice structures with minimal surfaces, International Journal of Mechanical Sciences 167 (2020).

[5] C. Yan, L. Hao, A. Hussein, P. Young, Ti-6Al-4V triply periodic minimal surface structures for bone implants fabricated via selective laser melting, J Mech Behav Biomed Mater 51 (2015) 61-73.

[6] B. Nagarajan, Z.H. Hu, X. Song, W. Zhai, J. Wei, Development of Micro Selective Laser Melting: The State of the Art and Future Perspectives, Engineering 5(4) (2019) 702-720.

[7] S. Rajagopalan, R.A. Robb, Schwarz meets Schwann: design and fabrication of biomorphic and durataxic tissue engineering scaffolds, Medical image analysis 10(5) (2006) 693-712.

[8] O. Al-Ketan, D.W. Lee, R. Rowshan, R.K. Abu Al-Rub, Functionally graded and multi-morphology sheet TPMS lattices: Design, manufacturing, and mechanical properties, J Mech Behav Biomed Mater 102 (2020) 103520.

[9] ISO 13314: 2011, Mechanical testing of metals—ductility testing—compression test for porous and cellular metals, International Organization for Standardization (2011).

[10] L.J. Gibson, M.F. Ashby, Cellular solids: structure and properties, Cambridge university press1999.